pubs.acs.org/acschemicalbiology

Articles

Clostridioides difficile TcdB Toxin Glucosylates Rho GTPase by an S_Ni Mechanism and Ion Pair Transition State

Ashleigh S. Paparella, Sean M. Cahill, Briana L. Aboulache, and Vern L. Schramm*

Cite This: *ACS Chem. Biol.* 2022, 17, 2507−2518

Read Online

ACCESS | Metrics & More | Article Recommendations | Supporting Information

ABSTRACT: Toxins TcdA and TcdB from *Clostridioides difficile* glucosylate human colon Rho GTPases. TcdA and TcdB glucosylation of RhoGTPases results in cytoskeletal changes, causing cell rounding and loss of intestinal integrity. Clostridial toxins TcdA and TcdB are proposed to catalyze glucosylation of Rho GTPases with retention of stereochemistry from UDP-glucose. We used kinetic isotope effects to analyze the mechanisms and transition-state structures of the glucohydrolase and glucosyltransferase activities of TcdB. TcdB catalyzes Rho GTPase glucosylation with retention of stereochemistry, while hydrolysis of UDP-glucose by TcdB causes inversion of stereochemistry. Kinetic analysis revealed TcdB glucosylation via the formation of a ternary complex with no intermediate, supporting an S_Ni mechanism with nucleophilic attack and leaving group departure occurring on the same face of the glucose ring. Kinetic isotope effects combined with quantum mechanical calculations revealed that the transition states of both glucohydrolase and glucosyltransferase activities of TcdB are highly dissociative. Specifically, the TcdB glucosyltransferase reaction proceeds via an S_Ni mechanism with the formation of a distinct oxocarbenium phosphate ion pair transition state where the glycosidic bond to the UDP leaving group breaks prior to attack of the threonine nucleophile from Rho GTPase.

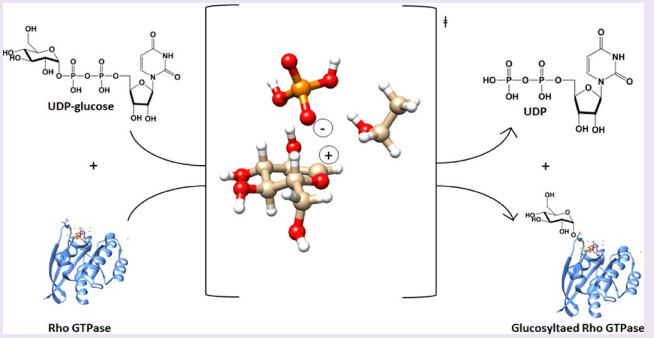

INTRODUCTION

Glycosyltransferases commonly catalyze glycosidic bond formation via the transfer of a sugar moiety from the activated nucleoside diphosphate sugar donor to acceptor substrates, including monosaccharides, polysaccharides, lipids, proteins, nucleic acids, and small organic molecules.[1] Glycosyltransferases can be classified as inverting or retaining depending on stereochemical outcome at the anomeric carbon.[1,2] Inverting glycosyltransferases use a single-displacement mechanism (S_N2) with a single oxocarbenium ion-like transition state. The inverting mechanism has been supported by mechanistic studies and kinetic isotope effect measurements.[1,3,4]

The reaction mechanism of retaining glycosyltransferases can occur by several proposed mechanisms (Figure 1).[1,5] Initially, retaining glycosyltransferases were proposed to proceed through double-displacement mechanisms, where an active site amino acid acts as a nucleophile, attacking the anomeric carbon to form a covalently linked glycosyl-enzyme intermediate before the deprotonated acceptor nucleophile can attack, resulting in retained stereochemistry of the newly formed glycosidic bond (Figure 1a).[1,5] However, retaining glycosyltransferases often lack a suitably positioned amino acid to act as the catalytic nucleophile.[1,5−11] Retention of stereochemistry without a covalently linked glycosyl-enzyme intermediate led to the proposal for an "internal return" S_Ni-like mechanism, where nucleophilic attack occurs at the same face as leaving group departure.[7,9,12−14] The S_Ni-like mechanism can proceed through a short-lived oxocarbenium ion intermediate (stepwise-mechanism) or a single oxocarbenium ion-like transition state (concerted mechanism) (Figure 1b, c).[5] The S_Ni mechanism has been supported by kinetic isotope effect (KIE) measurements on the solvolysis of glycosyl fluorides in hexafluoro-2-propanol which proposed a short-lived oxocarbenium ion pair intermediate.[15] KIE measurements have also been reported for trehalose-6-phosphate synthetase (OtsA), also supporting an S_Ni mechanism. However, the magnitude of the anomeric carbon KIE could not distinguish between stepwise and concerted S_Ni mechanisms.[16]

Recent quantum mechanics/molecular mechanics (QM/MM) studies have analyzed the retaining glycosyltransferases OtsA,[17] α-1,2-mannosyltransferase,[18] GalNAc-transferase 2,[19] mannoglycerate synthetase,[20] lipopolysaccharyl α-galactosyl transferase,[21] and glucosyl-3-phosphoglycerate synthetase.[11]

Received: May 9, 2022
Revised: August 11, 2022
Accepted: August 15, 2022
Published: August 29, 2022

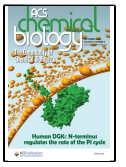

https://doi.org/10.1021/acschembio.2c00408
ACS Chem. Biol. 2022, 17, 2507−2518

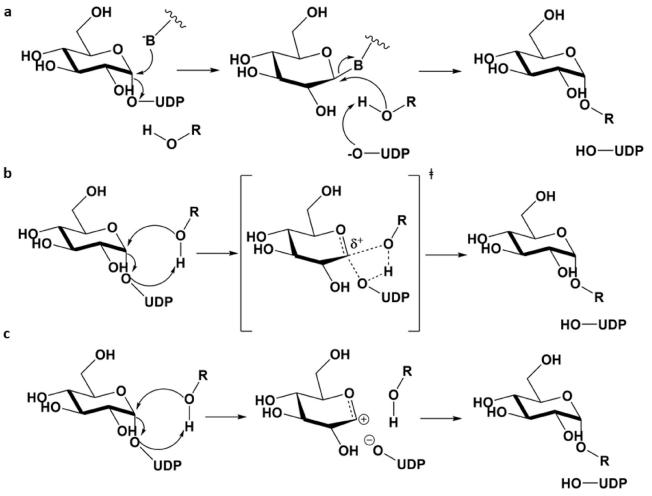

Figure 1. Proposed mechanisms for retaining glycosyltransferases: (a) Double displacement mechanism with the formation of covalently linked glycosyl intermediate. (b) Concerted S_Ni mechanism. (c) Stepwise S_Ni mechanism with the formation of the oxocarbenium-phosphate ion pair.

With the exception of lipopolysaccharyl α-galactosyl transferase, the enzymes were proposed to catalyze glycosylation via stepwise S_Ni mechanisms with short-lived oxocarbenium ion pair intermediates. These transition states were highly dissociative with the bond to the UDP leaving group being fully dissociated prior to nucleophilic attack. These studies suggest that the stepwise S_Ni mechanism is dominant for retaining glycosyltransferases.

Despite the wealth of knowledge for the glycosyltransferases, protein O-glucosyltransferases are less common. Here, we extend studies of glycosyltransferases to TcdB, a bacterial glucosyltransferase by the analysis of combined experimental KIEs and QM calculations.

The TcdA and TcdB toxins from *Clostridioides difficile* contain a glucosyltransferase (GT) domain that when processed and released from endosomes into the cytosol of mammalian cells glucosylate and inactivate Rho GTPases.[22−24] The TcdA and TcdB toxins are the primary determinants of *C. difficile* pathogenesis and as such are attractive therapeutic targets.[25−28] Detailed knowledge of the reaction mechanism and transition states of TcdA and TcdB defines reaction chemistry and is useful in the design of transition state analogues. TcdA and TcdB catalyze transfer of a glucosyl residue to a specific threonine residue in the switch I effector regions of Rho GTPases, including Rac1.[23] The glucosyltransferase domain of TcdA and TcdB belong to the GT44 family of glycosyltransferases, which also contains the bacterial toxin glucosyltransferases.[29] The TcdA and TcdB glucosyltransferase domains belong to the GT-A fold family of glycosyltransferases. The TcdA and TcdB glucosyltransferase domains show the highest catalytic activity in the presence of a combination of potassium, magnesium, and manganese ions.[30−32] Similar to other retaining glycosyltransferases, in the absence of an appropriately positioned acceptor to provide a catalytic nucleophile, the TcdA and TcdB toxins catalyze the slow hydrolysis of UDP-glucose.[32,33]

Previous KIE measurements on the glucohydrolase reactions of TcdA and TcdB demonstrated a highly dissociative glucocationic transition state. This information was used to identify the iminosugars isofagomine and noeuromycin as transition state analogue inhibitors.[33] Here, we characterize the mechanisms of both glucohydrolase (GH) and glucosyltransferase (GT) reactions of the TcdB GT domain. Retention of stereochemistry is confirmed for the TcdB GT reaction. In contrast, the TcdB GH reaction is demonstrated to proceed with the inversion of stereochemistry. Kinetic analysis of the TcdB GT reaction demonstrated that the reaction proceeds with the formation of a ternary complex. While positional isotope exchange analysis demonstrated that TcdB-catalyzed

Table 1. V/K KIEs, Intrinsic KIEs, Calculated KIEs, and Calculated EIEs for the TcdB-GTD Glucosyltransferase Reaction

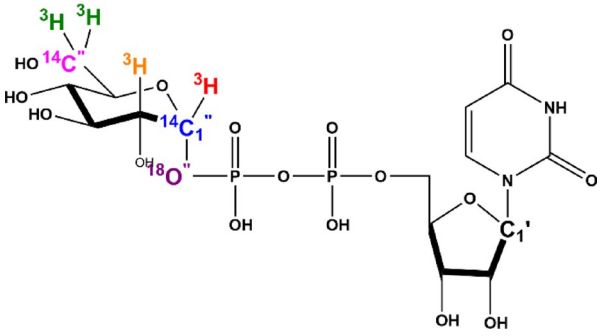

label	type of KIE[a]	experimental KIE TcdB-GTD	intrinsic KIE TcdB-GTD	calculated KIE TcdB-GTD	calculated EIE TcdB-GTD
1"-^{3}H	α-secondary	1.050 ± 0.002	1.064 ± 0.003	1.482	1.478
1"-^{14}C	primary label	1.009 ± 0.003	1.010 ± 0.001	1.012	1.011
1"-^{18}O	primary leaving group	1.028 ± 0.002	1.037 ± 0.002	1.039	1.018
2"-^{3}H	β-secondary	1.025 ± 0.001	1.032 ± 0.002	1.193	1.193
6"-^{3}H	remote label	1.056 ± 0.002	1.071 ± 0.002	N/A	N/A
6"-^{14}C	remote label	1.000	1.000	N/A	N/A

[a]Positions of isotopic labels in UDP-glucose designed for multiple KIE measurement and the resulting experimental and theoretical KIEs.

https://doi.org/10.1021/acschembio.2c00408
ACS Chem. Biol. 2022, 17, 2507−2518

glucosyltransfer occurs without reversible rotation of the leaving phosphoryl group.

KIE analysis combined with QM calculations support an S_Ni mechanism with an oxocarbenium ion pair transition state for the TcdB GT reaction. Knowledge of the TcdB GH and GT transition states is useful for the design of transition analogues with improved potency to act as antitoxins.

MATERIALS AND METHODS

Gene Expression and Protein Purification. Expression plasmid pET28a containing C-terminal His-6 tagged TcdB-GTD (amino acids 1−546) was kindly provided by Tam et al.[34] Conditions for the heterologous expression of TcdB-GTD in *Escherichia coli* (One Shot BL21 Star (DE3) cell line were adapted from Tam et al[34] and followed the method of Paparella et al.,[33] with purification by Ni-NTA chromatography and protein preparation in 20 mM Tris pH 7.5, 150 mM NaCl, 15% v/v glycerol, freezing, and storage at −80 °C.

Expression of Rac1 GTPase (amino acids 1−192) also followed the method of Paparella et al.[33] Expression from an open reading frame with an N-terminal His6 tag was cloned into pD454-SR:375415 (Atum Bio). Rac1 GTPase was expressed in *E. coli* (One shot BL21 Star, DE3 cell line), and recombinant protein expression was induced with 1 mM IPTG for 4 h at 30 °C. Purification of Rac1 was performed by Ni-NTA chromatography. The protein preparation was equilibrated in 20 mM Tris pH 7.5, 150 mM NaCl, 15% v/v glycerol for freezing and storage at −80 °C.

Synthesis of Isotopically Labeled Substrates. Isotopically labeled UDP-glucose was synthesized by coupled enzymatic reactions, as described previously.[33] In summary, individual 1-^{3}H, 2-^{3}H, 6-^{3}H, 1-^{14}C, 1-^{13}C, and 6-^{14}C labeled glucoses were used as starting materials to prepare 1″-^{3}H, 2-^{3}H, 6″-^{3}H, 1″-^{14}C, 1″-^{13}C, and 6″-^{14}C UDP-glucose, respectively (see Table 1). Synthesis from labeled glucose was accomplished by the sequential actions of hexokinase, pyruvate kinase, phosphoglucomutase, UDP-glucose pyrophosphorylase, and inorganic pyrophosphatase. Isotopically labeled UDP-glucoses were purified by Mono Q anion exchange HPLC in ammonium formate. Purity was established by coelution with commercially available UDP-glucose. 1″-^{18}O UDP-glucose and 1″-^{18}O, 1″-^{13}C UDP-glucose were prepared by oxygen exchange at the anomeric carbon in $H_2{}^{18}O$ (Cambridge isotope labs), detailed in the study of Paparella et al.[33,35] Isotopic enrichment of 1″-^{18}O, 1″-^{13}C UDP-glucose was assessed by mass spectrometry. Isotopic enrichment of 1″-^{18}O, 6″-^{14}C double labeled UDP-glucose, the isotope enrichment was assessed via mass spectrometry on a reaction without ^{14}C that was run in parallel. Isotope enrichment was determined to be >95%. Mass spectra were acquired on a Shimazu LCMS-2010EV spectrometer.

Stereochemistry of TcdB-GTD Glucohydrolase Reaction. The stereochemistry of the TcdB-GTD glucohydrolase reaction was monitored by nuclear magnetic resonance (NMR) spectroscopy. Reaction conditions were as follows: 50 mM HEPES pH 7.5, 100 mM KCl, 4 mM $MgCl_2$, 1 mM $MnCl_2$, 112.5 μM TcdB-GTD, and 10% D_2O. UDP-glucose was added to a final concentration of 20 mM, and the mixture was placed in a 3 mm NMR tube. The first NMR spectra was acquired 15 min after the addition of UDP-glucose. All NMR data were acquired at 25 °C using a Bruker AVIII 600 MHz spectrometer running TopSpin 3.6 and equipped with a 5 mm H/F-TCI cryogenic probe. The anomeric (C1′) cross peak volumes of α-D-glucose and β-D-glucose were determined in a 2D ^{1}H-^{13}C HSQC to monitor the rate of glucose formation coupled with the subsequent mutarotation that occurs with glucose in solution. Each HSQC timepoint was run for 10 min with 32 scans acquired for each increment using a spectral width of 14 and 80 ppm for ^{1}H and ^{13}C, respectively, and a recycle delay of 1 s. The data sets were collected using 2048 and 8 complex points for ^{1}H and ^{13}C, respectively, and the time-domain NMR data were linear predicted and zero filled in the indirect dimension and multiplied with a shifted sine-bell function (SSB = 2) in each dimension prior to Fourier transformation.

Stereochemistry of TcdB-GTD Glucosyltransferase Reaction. Stereochemistry of the TcdB-GTD glucosyltransferase reaction was assessed by NMR spectroscopy. Rac1 was purified as described above and glucosylated by TcdB-GTD using 1-^{13}C UDP-glucose. A glucosylation reaction was carried out for 90 min at room temperature and contained 50 mM HEPES pH 7.5, 100 mM KCl, 4 mM $MgCl_2$, 1 mM $MnCl_2$, 1 mM DTT, 200 μM 1-^{13}C UDP-glucose, 160 μM Rac1, and 0.5 μM TcdB-GTD. After 90 min, the solution was concentrated to 500 μL using a 10 kDa Amicon spin column. D_2O was added to a final concentration of 10% and transferred to a 5 mm NMR tube. The final concentration of Rac1 for NMR analysis was 280 μM. All NMR data were acquired at 25 °C using a Bruker AVIII 600 MHz spectrometer running TopSpin 3.6 and equipped with a 5 mm H/F-TCI cryogenic probe. A 2D ^{1}H-^{13}C HSQC was acquired to characterize the products. The HSQC was run for 16 h with 512 scans acquired for each increment using a spectral width of 12 and 80 ppm for ^{1}H and ^{13}C, respectively, and a recycle delay of 1.5 s. The data sets were collected using 2048 and 32 complex points for ^{1}H and ^{13}C, respectively, and the time-domain NMR data were linear-predicted and zero-filled in the indirect dimension and multiplied with a shifted sine-bell function (SSB = 2) in each dimension prior to Fourier transformation.

Kinetic Analysis of TcdB-GTD Glucosyltransferase Reaction. Initial reaction rate experiments for TcdB-GTD glucosytransferase activity were measured using 6-^{3}H UDP-glucose as a substrate and by capturing radiolabeled glucosylated Rac1 protein by the precipitation of the protein product using the method described in the study of Bensadoun and Weinstein[36] and Paparella et al.[33] Initial reaction rate studies used fixed UDP-glucose/6-^{3}H UDP-glucose or Rac1 at different concentrations while varying the concentrations of the other substrate. Terminated reaction samples were added to a precipitation mix of 120 μg/mL sodium deoxycholate, 6% trichloroacetic acid, and 10 μg/mL BSA. Samples were incubated at room temperature for 15 min before being centrifuged for 20 min at 13,000 rpm to separate the glucosylated protein product. The supernatant was removed, and the protein pellet was resuspended in 500 μL of 200 mM Tris−HCl pH 7.5, 5% SDS, and 20 mM NaOH. Samples were vortexed briefly and added to 20 mL scintillation vials to which 10 mL of Ultima Gold scintillation fluid was added (Perkin Elmer). The amount of glucosylated Rac1 was determined by scintillation counting of each sample for 1 min using a Tri-carb 2910TR scintillation counter (Perkin Elmer). The initial rates of the reaction were fit to the Michaelis Menten equation (eq 1), and a double-reciprocal Lineweaver−Burk plot was created. The data were best fit with a convergence of lines with a shared common x intercept.

$$v = \frac{V_{max} \times S}{K_m + S} \quad (1)$$

Positional Isotope Exchange Experiment. Reaction mixtures contained 50 mM HEPES pH 7.5, 100 mM KCl, 4 mM $MgCl_2$, 1 mM $MnCl_2$, 1 mM DTT, 500 μM [1-^{13}C, 1-^{18}O] UDP-glucose, 500 μM Rac1, and 0.1 μM TcdB-GTD. At 50, 100, 200, and 400 s, 150 μL aliquots of the reaction were added to 20 μL of 0.4 M EDTA (final concentration = 50 mM) to quench the reaction. This corresponded to 5, 20, and 40% conversion. Before NMR analysis, the reaction was diluted by 37% with D_2O, TSP was added as an internal chemical shift reference, and samples placed into 3 mm NMR tubes. NMR data was acquired at 25 °C using a Bruker AVIII 600 MHz spectrometer running TopSpin 3.6 and equipped with a 5 mm H/F-TCI cryogenic probe. The anomeric cross peak (C1′) of UDP-glucose was determined in a high-resolution 2D ^{1}H-^{13}C HSQC to resolve the cross-peak belonging to the C1′ bonded to ^{18}O from that bonded to ^{16}O expected to appear if positional isotope exchange (PIX) occurred during the enzymatic reaction. Each HSQC timepoint was run for 30 min with 8 scans acquired for each increment using a spectral width of 14 and 2 ppm for ^{1}H and ^{13}C, respectively, and a recycle delay of 1.1 s. The data sets were collected using 4096 and 128 complex points for ^{1}H and ^{13}C, respectively, and the time domain NMR data were linear-predicted in the indirect dimension and multiplied with a shifted sine-

https://doi.org/10.1021/acschembio.2c00408
ACS Chem. Biol. 2022, 17, 2507−2518

bell function (SSB = 3) in each dimension prior to Fourier transformation. The extent of the enzyme reaction was quantitated by 2D ^{1}H-^{13}C HSQC analysis of samples without enzymes and with enzymes to cause 40% reaction to quantitate the cross peak for glucosylated Rac1. Each HSQC was run for 9 h with 320 scans acquired for each increment using a spectral width of 12 and 80 ppm for ^{1}H and ^{13}C, respectively, and a recycle delay of 1.3 s. The data sets were collected using 4096 and 64 complex points for ^{1}H and ^{13}C, respectively, and the time-domain NMR data were linear-predicted in the indirect dimension and multiplied with a shifted sine-bell function (SSB = 2) in each dimension prior to Fourier transformation.

Attempted Glucocation Capture in the TcdB-GT Reaction. Reaction mixtures contained 50 mM HEPES pH 7.5, 100 mM KCl, 4 mM $MgCl_2$, 1 mM $MnCl_2$, 1 mM DTT, 500 μM [1-^{13}C] UDP-glucose, 500 μM Rac1, 5 μM TcdB-GTD, and 10% methanol. After reaction completion (2 h), proteins were removed by ultrafiltration (10 kDa Amicon spin column). The sample was made to 500 μL with 10% D_2O and transferred to a 5 mm NMR tube. NMR data were acquired as described for analysis of the TcdB-GTD glucosyltransferase reaction.

V/K KIEs for TcdB-GTD Glucosyltransferase Reaction. Measurements of V/K KIEs for the TcdB-GTD glucosyltransferase reaction were performed at room temperature using the competitive radiolabeled approach. Reaction conditions were as follows: 50 mM postassium phosphate, pH 6.0, 100 mM KCl, 4 mM $MgCl_2$, 1 mM $MnCl_2$, 1 mM DTT, 30 μM Rac1, 70 μM UDP-glucose ([*heavy label*] UDP-glucose + [*remote label*] UDP-glucose + unlabeled carrier), and 1 nM TcdB-GTD. For a typical KIE measurement, a master mix containing all reaction components (except enzyme) was prepared, and equal volume samples were aliquoted into tubes and designated as "control reactions," which include the no enzyme control and 3 replicates of the starting heavy/remote label ratio. TcdB-GTD was added to the remaining master mix, and the reaction was allowed to proceed to 10−20% completion. Equal volume aliquots of the TcdB-GTD reaction were added to the same volume of 100 mM EDTA pH 8.0 to quench the reaction. Labeled glucosylated Rac1 protein was precipitated as described above. Scintillation counting was performed on each sample over 10 cycles at 10 min/cycle using a Tri-carb 2910TR scintillation counter (Perkin Elmer). The dual channel instrument registers ^{3}H in channel A and ^{14}C in channels A and B. The raw data were analyzed to determine the total counts for ^{3}H-labeled glucosylated Rac1 and ^{14}C-labeled glucosylated Rac1. A control sample of ^{14}C-labeled glucose was used as a standard to establish the signal overlap between channel A and channel B for ^{14}C, as defined by eq 2:

$$r = \text{Channel A}/\text{Channel B} \tag{2}$$

Spectral deconvolution of the KIE data was achieved for ^{3}H and ^{14}C using eqs 3 and 4, respectively:

$$^{3}\text{H} = \text{Channel A} - (\text{Channel B} \times r) \tag{3}$$

$$^{14}\text{C} = \text{Channel B} + (\text{Channel B} \times r) \tag{4}$$

V/K KIE values were calculated from eq 5, where R_0 and R_f are the ratios of [heavy label] UDP-glucose to [remote label] UDP-glucose prior to the reaction and at partial conversion, respectively, and f is the fraction of substrate conversion for KIE measurements involving 1″-^{14}C, 1″-^{18}O, and 6″-^{14}C UDP-glucose:

$$\text{KIE}_{V/K} = \frac{\text{Log}(1-f)}{\text{Log}\left(1 - f\frac{R_f}{R_0}\right)} \tag{5}$$

The observed KIE values were corrected for the 6″-^{3}H remote isotope effect using eq 6:

$$\text{KIE} = \text{KIE observed} \times 6 - {}^{3}\text{H KIE} \tag{6}$$

TcdB-GTD Glucosyltransferase Forward Commitment. Forward commitment for UDP-glucose in the TcdB-GTD glucosyltransferase reaction was measured using the isotope trapping method.[37] A 50 μL sample of the TcdB-GTD:UDP-glucose equilibrium complex was formed by incubating 5 μM TcdB-GTD with 70 μM 6″-^{14}C UDP-glucose for 5 s in 50 mM phosphate pH 6.0, 100 mM KCl, 4 mM $MgCl_2$, 1 mM $MnCl_2$, and 1 mM DTT at room temperature. A chase solution (450 μL of 5 mM unlabeled UDP-glucose, 30 μM Rac1, 50 mM phosphate buffer pH 6.0, 100 mM KCl, 4 mM $MgCl_2$, 1 mM $MnCl_2$, and 1 mM DTT) was rapidly mixed with the ES complex solution, and 4 × 50 μL aliquots were removed from the mixture and quenched with 50 μL of 100 mM EDTA pH 8.0 at 5, 10, 15, and 20 s after addition of chase solution. Control reactions containing no enzyme were processed in parallel to correct for background levels. Labeled glucosylated Rac1 protein was precipitated as described above. Scintillation counting was performed as described for KIE measurements. The amount of glucosylated Rac1 produced after the addition of chase solution was plotted as a function of time and extrapolated to time = 0. The concentration of the enzyme substrate (ES) complex was calculated using eq 7, where E represents the enzyme concentration, S represents the concentration of 6″-^{14}C UDP-glucose, and K_M is the Michaelis constant for UDP-glucose in the TcdB-GTD glucosyltransferase reaction.

$$\text{ES} = (ES)/(S + K_M) \tag{7}$$

C_f was calculated using eq 8, where Y is the ratio of moles of glucose product P (y-intercept at x = 0) per mole of the TcdB-GTD:UDP-glucose ES complex (eq 9).

$$C_f = Y/(1 - Y) \tag{8}$$

$$Y = P/\text{ES} \tag{9}$$

Solvent KIE. A solvent KIE for the TcdB-GTD glucosyltransferase activity was measured using the TcdB-GTD glucosyltransferase assay described above for V/K KIE measurements. Reactions were carried out in 0, 16, 32, 49, 65, and 82% D_2O. Glucosylated Rac1 was isolated using the protein precipitation method described above. Initial rates were used to calculate the solvent KIE using eq 10, where k is the reaction rate, n is the atom fraction of deuterium, and C is commitment to catalysis. The intrinsic solvent KIE was calculated from the term $1/\phi_3^T$.

$$\frac{k_n}{k_{E,0}} = \frac{(1 + C)(1 - n + n\phi_3^T)}{1 + C(1 - n + n\phi_3^T)} \tag{10}$$

Computational Methods. Glucohydrolase and glucosyltransferase transition state structures for TcdB-GTD were determined from the experimentally measured intrinsic KIE values as constraints for theoretical transition state structures determined via density functional theory in Gaussian 09 using the B3LYP level of theory and the 6-31 g(d) basis set.[38] Calculated KIE values for theoretical transition states were calculated at 25 °C (TKELV = 298.15) using ISOEFF98[39] from scaled vibrational frequencies (SCFACT = 0.977) of optimized structures of UDP-glucose in the ground state and each transition state.

For TcdB-GTD glucosyltransferase transition state calculations, a modified threonine acceptor nucleophile was included in optimized structures of the transition state. The input coordinates for the optimization of UDP-glucose in the ground state were taken from the x-ray crystal structure of the TcdA-GTD in complex with UDP-glucose (PDB ID: 3SRZ). The fully elaborated UDP-glucose structure was truncated to glucose-1-PO_4. Truncation of reactants for Gaussian calculations (glucose-1-PO_4 and a cut-off threonine nucleophile) differs for the reality of the UDP-Mg^{2+} and UDP-Mn^{2+} leaving groups, resulting from the combined use of Mg^{2+} and Mn^{2+} in KIE experiments. Thus, the leaving group potential of the calculated and actual leaving groups should be noted. All structures were assigned a formal charge of 0 and a multiplicity of 1. The optimized ground-state structure was located as the global minimum and displayed no imaginary frequencies.

For the TcdB-GTD glucohydrolase reaction, initial transition state calculations were performed by fixing the 1−C−1−O(P_i) and 1−C−O(H_2O) bonds and varying their lengths from 1.8 to 3.0 Å in 0.2 Å

https://doi.org/10.1021/acschembio.2c00408
ACS Chem. Biol. 2022, 17, 2507−2518

increments. Transition state structures were refined from the results of the first calculation by varying the 1−C−1−O(P_i) bond length from 2.2 to 2.4 Å in 0.01 Å increments while keeping the 1−C−O(H_2O) bond length fixed at 2.2 Å. The final transition state structure had a single imaginary frequency. For the TcdB-GTD glucohydrolase reaction, a stepwise S_Ni mechanism was investigated, where the 1−C−1−O(P_i) bond was fixed at 3.0 Å and the 1−C−O(Thr) and 1−O(P_i)−H(Thr) bonds were fixed and varied from 1.8 to 3.0 Å in 0.2 Å increments. The final transition state structure was consistent with a distinct oxocarbenium ion intermediate. Equilibrium isotope effects (EIEs) for the intermediate were calculated with ISOEFF98 using the optimized structure of the UDP-glucose ground state and the oxocarbenium ion. Electrostatic potential maps for the TcdB-GTD glucohydrolase and glucosyltransferase ground state and transition state structures were visualized in GaussView 6.0 (isovalue = 0.04) from the electron density and potential cubes acquired from the checkpoint files of the geometry optimization and frequency calculations.

RESULTS AND DISCUSSION

Stereochemistry of TcdB Glucohydrolase and Glucosyltransferase Reactions. Transition state analysis of the TcdB glucosyltransferase domain (TcdB-GTD) was aided by the stereochemical outcome of the TcdB-GTD GH and GT reactions. We used 2D ^{1}H-^{13}C HSQC NMR spectroscopy to monitor the formation of α-D-glucose or β-D-glucose from TcdB catalyzed hydrolysis of UDP-glucose. However, D-glucose mutarotates between α- and β-anomeric forms with an equilibrium mixture of 36% α-D-glucose and 64% of β-D-glucose at physiological pH values.[40] The mutarotation of glucose in aqueous solution reaches equilibrium in approximately 2 hours.[41−43] For α-D-glucose and β-D-glucose, the ^{13}C1-^{1}H anomeric peaks are found at approximately 5.3 and 4.7 ppm, respectively. TcdB-GTD (112.5 μM) and UDP-glucose (20 mM) were incubated at 25 °C, and NMR spectra were acquired 15 min after enzyme addition (approximately 90 turnovers). At this early time point, the anomeric carbon peak ratio corresponding to β-D-glucose/α-D-glucose = 3.9. Following equilibration of the glucose product at 180 min, the ratio stabilized at β-D-glucose/α-D-glucose = 1.4 (Figures 2a and S1). The TcdB-GTD GH reaction results in the formation of β-D-glucose, establishing inversion of stereochemistry for TcdB-GTD GH activity.

Stereochemical outcome of the TcdB-GTD GT reaction was monitored by 2D ^{1}H-^{13}C HSQC NMR for formation of the C1-H anomeric peak of the glucosylated Rho GTPase acceptor protein (Rac1). Based on earlier reports of the related *C. sordellii* lethal toxin, also a member of the large clostridial toxins, we anticipated TcdB-GTD to catalyze glucosylation of Rho GTPases with retention of stereochemistry.[43,45] TcdB-GTD was incubated with Rac1 and [1-^{13}C glucose]UDP-glucose, and the C1-H anomeric peak corresponding to glucosylated threonine of Rac1 was monitored (Figure 2b). The peak corresponding to the C1-H anomeric peak of glucosylated Rac1 appeared at approximately 5.0 ppm, consistent with previous studies.[44] As controls, we acquired spectra of α-methyl-glucoside, β-methyl-glucoside, and α-glucosylated threonine. The overlay of the NMR spectra indicates α-glucosylated threonine, thus confirming retention of stereochemistry for the TcdB-GTD GT reaction (Figure 2b).

Kinetics of the TcdB Glucosyltransferase Reaction. Retention of stereochemistry for the TcdB-GTD GT reaction implies a double-displacement mechanism or an S_Ni mechanism. Steady state kinetic mechanisms can indicate whether TcdB GT activity proceeds via a double displacement mechanism with a covalent intermediate or through a sequential mechanism with ternary complex formation.[46] Steady state kinetic measurements on the TcdB-GTD GT reaction were used to distinguish between these mechanisms. Double displacement mechanisms predict double reciprocal plots with varied substrates to be parallel lines while for a sequential mechanism (S_Ni) with ternary complex formation, the lines on the double reciprocal plot intersect on the left of the *x*-axis.[47] A sequential mechanism would support TcdB glucosyltransfer via an S_Ni mechanism. Double reciprocal plots indicated a sequential mechanism, indicating that both UDP-glucose and Rac1 need to bind to TcdB-GTD, forming a ternary complex before reacting through an S_Ni mechanism (Figure 3). It has been proposed that TcdB-GTD binds to UDP-glucose prior to Rac1 binding, as indicated by X-ray crystal structures of TcdA-GTD in complex with UDP and a recently published crystal structure of the TcdB-GTD:Cdc42:UDP complex.[47,48]

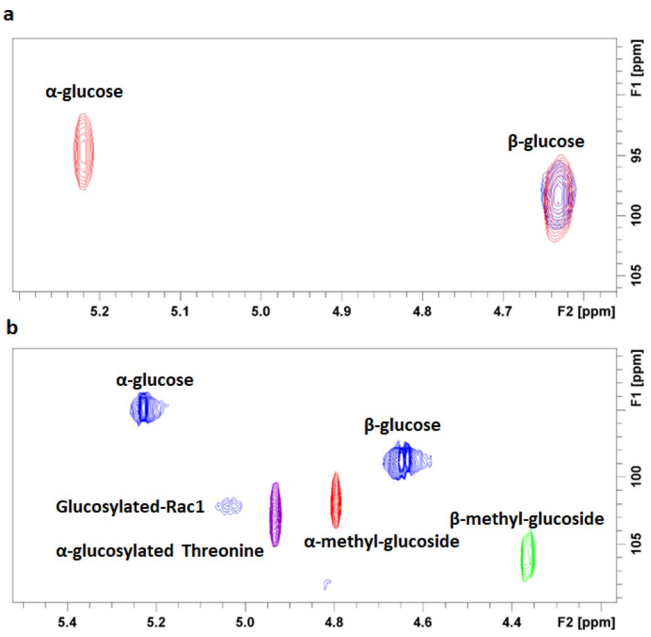

Figure 2. NMR analysis of stereochemistry of TcdB-GTD glucohydrolase and glucosyltransferase reactions: (a) 2D ^{1}H-^{13}C HSQC spectrum was enriched in β-D-glucose early in the TcdB-GTD glucohydrolase reaction (blue) relative to mutarotation equilibrium (red). (b) 2D ^{1}H-^{13}C HSQC spectrum for the C1' anomeric carbon of glucosylated Rac1 formed in the TcdB-GTD glucosyltransferase reaction. The C1 and C1' anomeric carbons of α-glucose, β-glucose, α-methyl-glucoside, β-methyl-glucoside, and α-glucosylated threonine are indicated.

Positional Isotope Exchange. The chemical steps of the TcdB-GTD GT reaction were analyzed by ^{18}O-UDP-[^{13}C]-glucose PIX experiments. PIX experiments detect reversible enzyme reaction steps and can indicate the lifetimes of potential intermediates.[3] The S_Ni mechanism suggests loss of the bond to UDP prior to attack by the incoming threonine nucleophile. If there is a stabilized glucocation intermediate, the β-phosphoryl group of UDP may be free to rotate, recombine with the glucocation, and equilibrate with the substrate UDP-glucose, to exchange the bridging phosphoryl ^{18}O for ^{16}O (Figure 4a). Chemical reversibility for an

https://doi.org/10.1021/acschembio.2c00408
ACS Chem. Biol. 2022, 17, 2507−2518

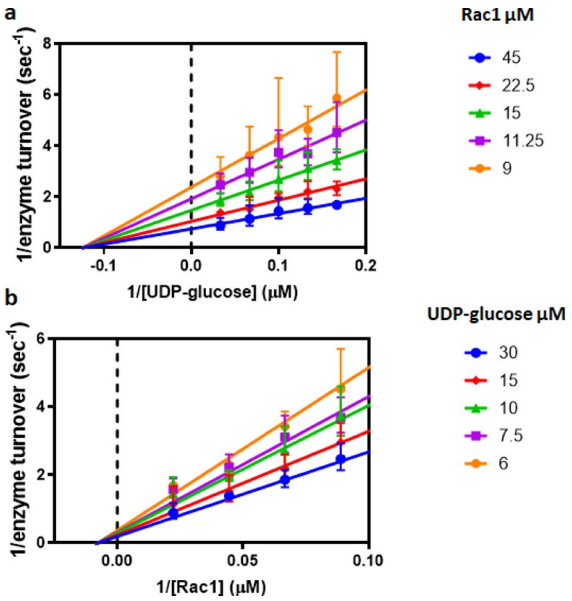

Figure 3. Steady state kinetic measurements on the TcdB-GTD glucosyltransferase reaction. Initial rates were fit to the Michaelis–Menten equation, and double reciprocal plots show lines intersecting on the *x*-axis. (a) Varying UDP-glucose concentrations at fixed Rac1 concentrations. (b) Varying Rac1 concentrations at fixed UDP-glucose concentrations.

oxocarbenium ion pair intermediate in the GT reaction of TcdB-GTD is tested by this PIX experiment.

Double-labeled [1″-^{13}C, bridge-β-^{18}O]UDP-glucose was synthesized to test for PIX in the TcdB reaction. The presence of the ^{18}O label at the bridging position causes an upfield ^{13}C NMR shift in the doublet from 98.33/98.38 to 98.30/98.35 ppm relative to ^{16}O label at the bridging position (Figure 4c). The anomeric carbon is split into a doublet because it is coupled to the ^{31}P via ^{2}J (^{13}C, ^{31}P) scalar coupling – ^{31}P is spin 1/2, causing the ^{13}C signal to split.

TcdB-GTD was incubated with excess [1″-^{13}C, 1″-^{18}O]UDP-glucose and Rac1, and samples were quenched at 5, 20, and 40% conversion to UDP and glucosylated Rac1. For each sample, no shift in the UDP-glucose anomeric carbon peaks were detected (Figure 4), indicating that no PIX occurs for the TcdB-GTD GT reaction. Thus, the ^{18}O label does not scramble from the bridging to the nonbridging position during the glucosyltransferase reaction.

A lack of PIX exchange establishes that the glucocation formed in the reaction chemistry is not free to permit β-phosphoryl rotation and reversible reaction to reform UDP-glucose. Chemical possibilities are that glucosyl loss is not complete prior to attack of the nucleophilic threonine of Rac1 and/or the β-phosphate of the UDP leaving group is restricted in the catalytic site and not free to rotate and/or that the glucocation transition state has low bond orders to both the leaving group and attacking nucleophile, but its lifetime is too short to permit phosphoryl rotational equilibrium. This result is consistent with other retaining glycosyltransferases including galactosyltransferase,[3] glycogen synthase,[49] and sucrose synthetase,[50] where no PIX effect has been reported.

Attempted Glucocation Capture. PIX analysis suggested a glucocationic transition state too sequestered to too short-lived to permit rotational equilibration of the β-phosphoryl group of UDP-glucose. An independent analysis of the presence of a stabilized glucocation is its reactivity (capture) by small nucleophiles. Capture of an oxocarbenium ion intermediate was attempted in the TcdB-GTD GT reaction

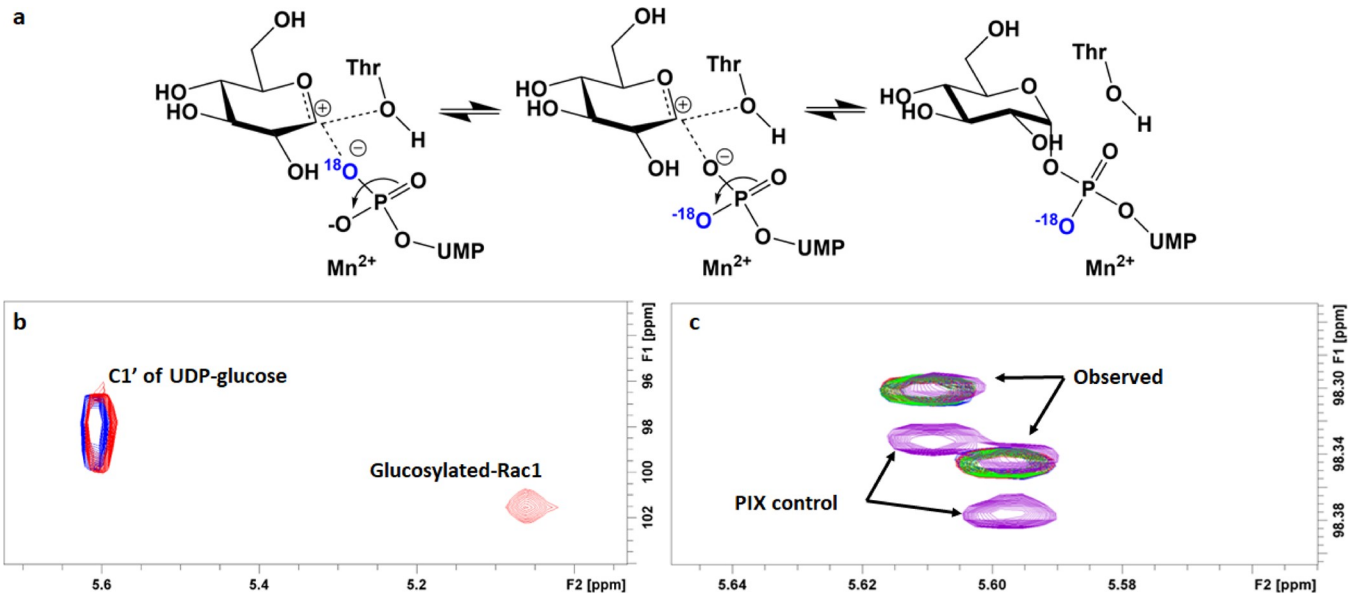

Figure 4. Positional isotope exchange analysis of TcdB glucosyltransferase: (a) Positional isotope exchange reaction scheme. A glucocation with sufficient lifetime permits the weakly-bonded β-phosphoryl group of UDP-glucose to rotate and return to the reactant state with reposition of the bridging ^{18}O to nonbridging ^{18}O with a consequent NMR shift of the ^{13}C-glucose anomeric carbon. (b) 2D ^{1}H-^{13}C HSQC spectrum demonstrating the transfer of glucose from UDP-glucose to form glucosyltated Rac1. Red is TcdB-GTD glucosyltransferase products at 40% completion and blue is the no enzyme control. c) 2D ^{1}H-^{13}C HSQC spectrum showing the anomeric ^{13}C1′ carbon of [^{13}C1′-bridge-^{18}O]UDP-glucose from the TcdB-GTD glucosyltransferase reaction quenched at 5% (blue), 20% (red), and 40% (green) completion. A TcdB-GTD glucosyltransferase reaction quenched at 40% completion (observed). As a PIX control for observation to nonbridge-^{18}O, the 2D ^{1}H-^{13}C HSQC spectrum of unlabeled UDP-glucose is compared (purple).

https://doi.org/10.1021/acschembio.2c00408
ACS Chem. Biol. 2022, 17, 2507–2518

Table 2. Summary of V/K KIEs, Intrinsic KIEs and Calculated KIEs from QM Calculations for the TcdB-GTD Glucohydrolase Reaction

label[a]	type of KIE	experimental KIE TcdB-GTD[b]	intrinsic KIE TcdB-GTD[c]	calculated KIE TcdB-GTD
1"-^{3}H	α-secondary	1.203 ± 0.001	1.216 ± 0.001	1.218
1"-^{14}C	primary label	1.042 ± 0.001	1.045 ± 0.001	1.066
1"-^{18}O	primary leaving group	1.026 ± 0.002	1.027 ± 0.002	1.025
2"-^{3}H	β-secondary	1.012 ± 0.001	1.014 ± 0.001	1.014
6"-^{3}H	remote label	1.053 ± 0.001	1.056 ± 0.001	N/A
6"-^{14}C	remote label	1.000	1.000	N/A

[a]Positions of isotopic labels in the substrate UDP-glucose designed for multiple KIE measurement and the resulting experimental and theoretical KIEs. Colored labels correspond to those of Table 1. [b]Experimental and intrinsic KIEs were previously measured and taken from ref 28. Six independent measurements were performed for each KIE, and the data represent the mean values ± SEM. [c]Experimental KIEs were corrected for forward commitment (eqs 7−9) to give intrinsic KIE values. The remote 6″-^{14}C value of unity provides the standard unity reference for all other isotope effects.

in the presence of 10% methanol. An oxocarbenium ion intermediate with lifetime and geometry to permit diffusional approach will react with methanol as a nucleophilic acceptor to form α-methyl or β-methyl glucose. No methyl-glucose was detected (Figures 2 and S2). Consistent with PIX, the TcdB-GTD GT reaction does not contain an oxocarbenium ion pair with a chemically reactive environment or reversible exchange.

KIE on the TcdB Glucosyltransferase Reaction. A glucosyltransfer S_Ni mechanism can proceed through an oxocarbenium ion intermediate or a concerted mechanism with bond making to the Rac1 threonine simultaneous with loss of the UDP leaving group. We measured KIEs on the TcdB-GTD GT reaction to resolve these differences. KIEs were measured using the competitive radiolabeled approach with isotopically labeled UDP-glucose substrates. This method yields (V/K) KIEs, which report on all steps from substrate binding up to and including the first irreversible chemical step.[51,52] For the TcdB-GTD GT reaction, departure of the UDP leaving group is considered to be irreversible, as reversal of enzyme-bound UDP would result in PIX exchange. Experimental KIEs can be altered or obscured by forward commitment factors (C_f). However, intrinsic KIEs that reflect only the chemical step are required to provide transition state information. Correction of experimental KIEs to intrinsic KIEs involves the measurement of commitment factors, the probability that molecules in the Michaelis complex will partition to product or be released to the unreacted substrate pool. Experimental KIEs on the TcdB-GTD GT reaction with excess Rac1 and UDP-glucose concentrations at physiological pH resulted in KIEs close to unity, indicating significant forward commitment (data not shown). Therefore, we measured the forward commitment factor associated with the TcdB-GTD GT reaction using the substrate trapping method developed by Rose.[37] The forward commitment factor was measured to be 0.285 ± 0.012 and was used to correct the measured KIEs for the TcdB-GTD GT reaction (Figure S3).

UDP-glucose was synthesized enzymatically or chemo-enzymatically from appropriately labeled glucose as the starting material to yield [1″-^{3}H], [2″-^{3}H], [1″-^{14}C], [1″-^{18}O 6″-^{14}C], [6″-^{3}H], and [6″-^{14}C]UDP-glucose substrates (Figure S4). [6″-^{14}C]Glucose locates the heavy atom 3 bonds away from the anomeric carbon, a position where ^{14}C KIE is known to be unity and therefore served as the reference. Therefore, [1″-^{3}H], [2″-^{3}H], and [6″-^{3}H] KIEs were measured in pairs with [6″-^{14}C]UDP-glucose serving as the control (Table 1). KIEs for [1″-^{14}C], [1″-^{18}O 6″-^{14}C], and [6″-^{14}C] were measured in pairs with [6″-^{3}H]UDP-glucose serving as the remote label and were corrected for [6″-^{3}H] remote effects by the latter (Table 1 and Figure S4). Previously reported intrinsic KIEs for the TcdB-GTD GH reaction are also shown for comparison (Table 2).[33]

The [1″-^{14}C] primary KIE reports on bonding and reaction coordinate motion of the anomeric carbon at the transition state. This isotope effect is typically 1.00−1.02 (k_{light}/k_{heavy}) for an S_N1 mechanism with a discrete oxocarbenium ion transition state, 1.025−1.06 for an S_N1-like concerted mechanism with partial bonds remaining to the anomeric carbon at the transition state, and 1.06−1.16 for an S_N2 associative concerted mechanism.[53] The [1″-^{14}C] KIE was 1.010 ± 0.001, indicating the presence of an oxocarbenium ion pair between the anionic UDP leaving group oxygen and the cationic anomeric carbon, thereby supporting an S_Ni mechanism with an oxocarbenium ion transition state.

The [1″-^{18}O] primary KIE reports on the extent of cleavage of the UDP-glucose glycosidic bond at the transition state. The [1″-^{18}O] KIE for the TcdB-GTD GT reaction was measured to be 1.037 ± 0.002. A fully cleaved glycosidic bond to generate an anionic leaving group is expected to generate a maximum KIE of 1.047.[54] For TcdB-GTD, the KIE indicates substantial cleavage of the UDP-glucose glycosidic bond at the transition state. The magnitude of the TcdB-GTD [1″-^{18}O] KIE could also reflect full departure of the UDP leaving group with partial protonation of the departing oxygen, a transition state structure precedented by trehalose-6-phosphate synthetase (OtsA).[15] Therefore, the [1″-^{18}O] KIE for the TcdB-GTD GT reaction is interpreted to reflect substantial leaving group bond cleavage with partial protonation of the leaving group oxygen.

The α-secondary [1″-^{3}H] KIE reports on the changes in bond hybridization at the anomeric carbon (sp^3 vs sp^2) reflecting the degree of oxocarbenium ion character at the transition state.[53,55] An sp^2 geometry at the transition state creates out-of-plane bending freedom of the hydrogen atom, generating a normal isotope effect. The [1″-^{3}H] KIE was measured to be 1.064 ± 0.003. Oxocarbenium ionlike transition states typically result in α-secondary KIEs of magnitude >1.15.[53,55] In comparison, the [1″-^{3}H] KIE for the TcdB-GTD GH reaction was measured to be 1.216, and for the retaining glycosyltransferase OtsA, the α-secondary KIE

https://doi.org/10.1021/acschembio.2c00408
ACS Chem. Biol. 2022, 17, 2507−2518

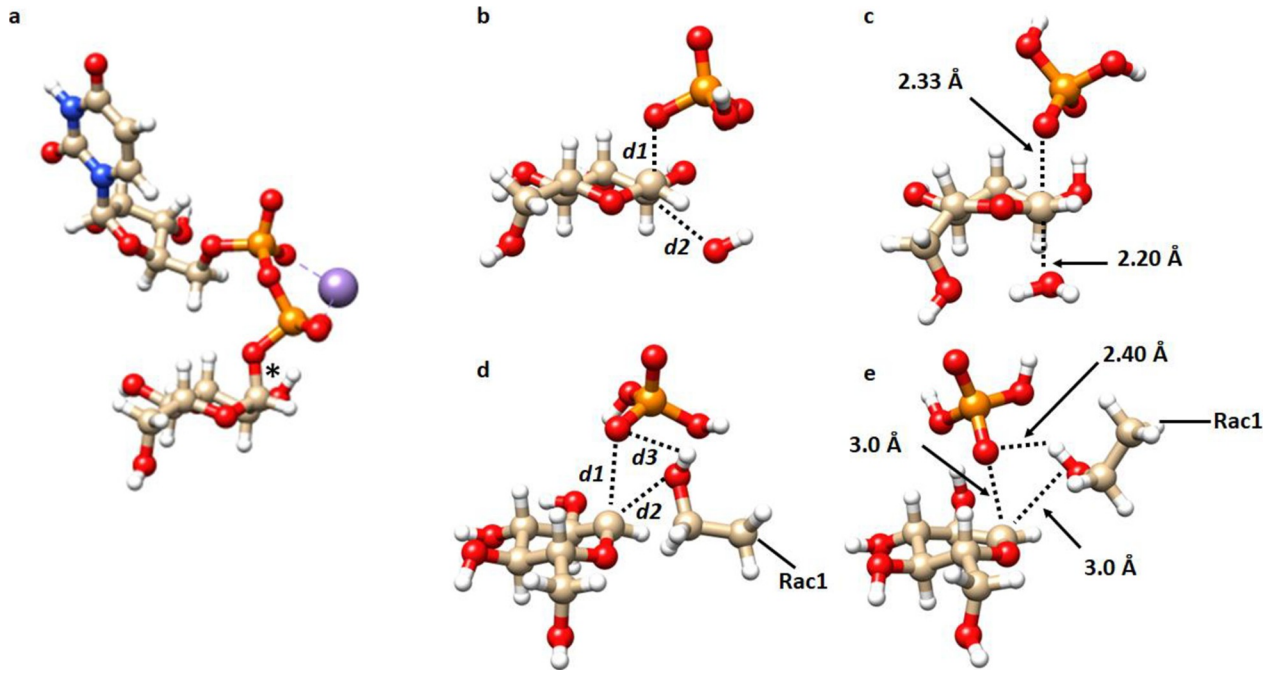

Figure 5. Optimized ground state and transition structures for TcdB glucohydrolase and glucosyltransferase reactions. (a) UDP-glucose structure is taken from PDB 3SRZ. The glycosidic bond is indicated by an asterisk. (b) Cut-off model for the ground state used to model the TcdB-GTD glucohydrolase transition state structure. Calculations were made by varying the lengths of the C−O bonds indicated by *d*1 and *d*2. (c) Calculated TcdB-GTD glucohydrolase transition state structure where calculated KIEs provided the best fit to experimental KIEs. (d) Cut-off model for the optimized ground state structure used to model the TcdB-GTD glucosyltransferase transition state. Calculations fixed the C−O bond (*d*1) at 3.0 Å and varied the lengths of the C−O bond and O−H bonds (*d*2 and *d*3, respectively). (e) Calculated TcdB-GTD glucosyltransferase transition state where the theoretical and intrinsic KIEs were in the best agreement.

is reported to be 1.284.[16] The relatively small α-secondary KIE for the TcdB-GTD GT reaction could reflect a crowded environment at the transition state, where the out-of-plane bending mode that would normally occur for an sp^2 hydrogen atom is restricted by the encroaching Rac1 threonine acceptor nucleophile.

The β-secondary [2″-^{3}H] KIE reports on the degree of hyperconjugation between the σ(C−H) orbital at C2 to the σ^*(C−O) orbital from the anomeric carbon to the UDP leaving group.[53,56] The [2″-^{3}H] KIE for the TcdB-GTD GT reaction of 1.032 ± 0.002 suggests that the C2−H2 bond is near-perpendicular to the C1-UDP bond at the transition state.[56] β-secondary KIEs of magnitude >1.07 have been reported for other N-glycohydrolases and glycosyltransferases with oxocarbenium ion-like transition states.[16,53] As the primary [1″-^{14}C] and [1″-^{18}O] KIEs support an oxocarbenium ionlike transition state, the [2″-^{3}H] KIE reflects an unusual transition state geometry with little hyperconjugation from the σ(C−H) orbital at C2″. Oxocarbenium ion transition states are expected to generate C5-O5-C1-C2 atoms of the glucose ring in a near coplanar geometry. Four possible conformations of the hexopyranose ring can accommodate the co-planar arrangement, ^{2,5}B, $B_{2,5}$, $^3H_4$, and $^4H_3$ (Figure S5). Of the four possible structures, only the $B_{2,5}$ hexopyranose structure is consistent with the small β-secondary KIEs.[12,57] The $B_{2,5}$ hexopyranose structure is likely to be a feature of the transition state geometry based on the small β-secondary [2″-^{3}H] KIE of (1.014) for the TcdB-GTD GH reaction.

A remote [6″-^{3}H] KIE was measured to be 1.071 ± 0.002 for the TcdB-GTD GT reaction. Remote tritium binding isotope effects contribute to V/K isotope effects and typically arise from enzyme-induced distortion of the sp^3 geometry at C6″. This is a common feature among GH and GT enzymes. A similar remote tritium KIE was also observed for the TcdB-GTD GH reaction (Table 2).[52,53]

The solvent deuterium KIE for the TcdB-GTD GT reaction was measured in the presence of varying amounts of D_2O. The solvent KIE was calculated to be 2.24 ± 0.15 and a linear function of deuterium concentration. A single proton transfer occurring at the TcdB-GTD GT transition state is indicated (Figure S6).

Kinetic analysis and the KIEs support an S_Ni mechanism that occurs via an oxocarbenium ion pair transition state. Unusually small α-secondary and β-secondary KIEs are attributed to a $B_{2,5}$ hexopyranose geometry and restricted environment for the ternary complex at the transition state.

Computational Analysis of the TcdB Glucohydrolase and Glucosyltransferase Transition States. Transition states for the TcdB-GTD GH and GT reactions were modeled using the experimental intrinsic KIEs as constraints for computational chemistry. Geometry for the transition state calculations used the initial coordinates for UDP-glucose (ground state) taken from a crystal structure of the TcdA GT domain in complex with UDP-glucose (PDB ID: 3SRZ). A simplified atomic cutoff model containing 29 atoms was used in the calculations. For optimization of the GH transition state structure, a water molecule was included on the β-face of glucose (32 atoms) (Figure 5b). Currently, there is no available structure of the ternary complex of TcdB-GTD in complex with UDP-glucose and an acceptor Rho GTPase protein. Although a structure of a TcdB-GTD:Cdc42:UDP complex has been recently published, glucose is absent as UDP-glucose was hydrolyzed during crystallization.[48] Analysis of the GT transition state included a truncated nucleophilic

https://doi.org/10.1021/acschembio.2c00408
ACS Chem. Biol. 2022, 17, 2507−2518

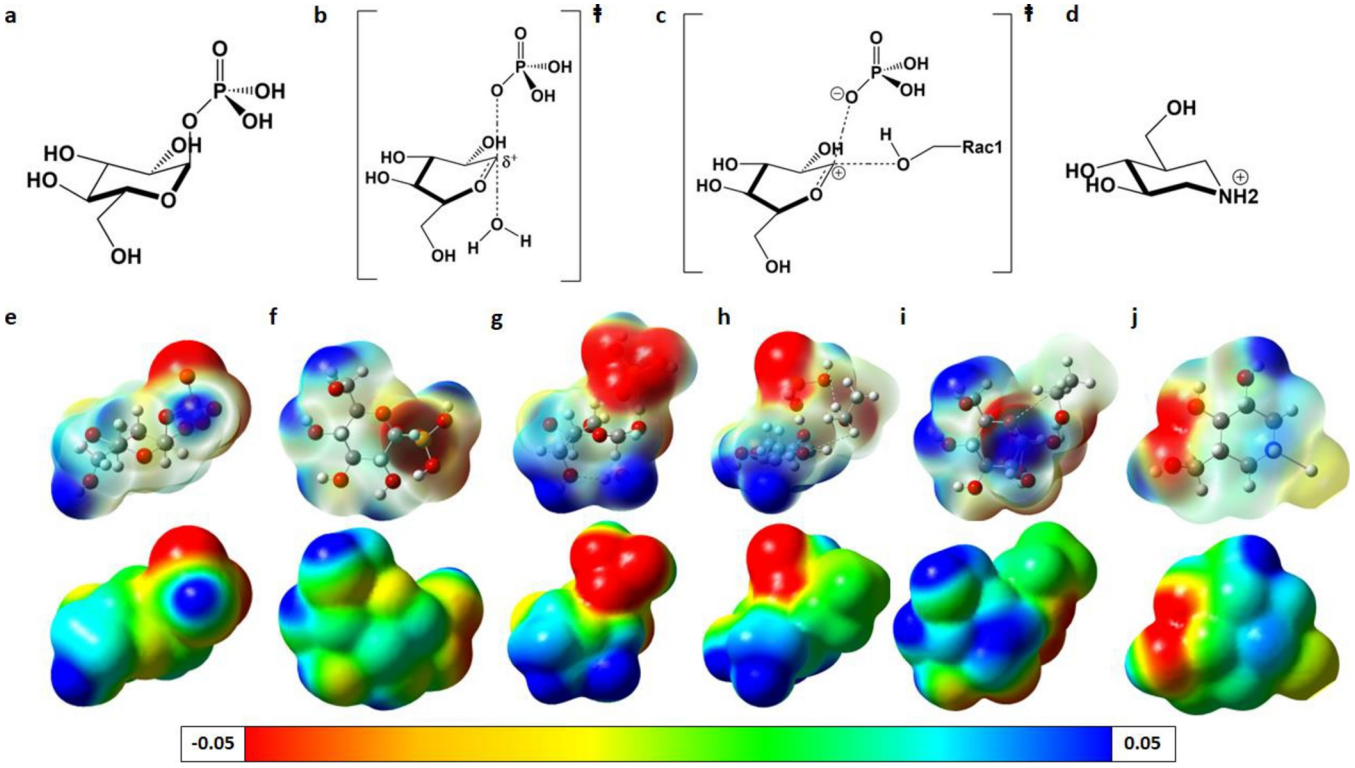

Figure 6. Structures and electrostatic potential surfaces for the TcdB-GTD ground state, GH and GT transition states and isofagomine, a TcdB-GTD transition state analogue. Chemical structures are shown on top and are the (a) TcdB-GTD ground state. (b) TcdB-GTD GH transition state. (c) TcdB-GTD GT transition state. (d) Protonated isofagomine. Geometric and electrostatic potential surfaces (EPS) maps for the TcdB-GTD ground state and transition state structures and transition state analogue, isofagomine are shown in panels e to j. Electron-rich charge is red, and electron-deficient charge is blue. Transparent EPS maps with imbedded structures are as follows: (e) TcdB-GTD ground state, (f) view of the anomeric carbon from the β-face of glucose. (g) TcdB-GTD glucohydrolase transition state structure, (h) TcdB-GTD glucosyltransferase transition state structure, (i) TcdB-GTD glucosyltransferase transition state structure viewed from the anomeric carbon on the β-face of glucose, and (j) structure of the transition state analogue isofagomine with view of the protonated nitrogen atom.

threonine side chain placed on the α-face of the glucose ring (38 atoms) (Figure 5d). Calculations were performed in Gaussian 09 using the B3LYP level of theory and the 6-31g(d) basis set.[38]

Theoretical transition states for the TcdB-GTD GH reaction were generated by varying the lengths of the C−O bond between the anomeric carbon and phosphate leaving group and the C−O bond between the anomeric carbon and incoming water nucleophile, marked as *d*1 and *d*2, respectively (Figure 5b). Theoretical KIEs for each potential transition state were calculated from scaled vibrational frequencies in ISOEFF98.[39] Bond lengths from the anomeric carbon to the phosphate leaving group or to the incoming nucleophilic water were varied from 1.8−3.0 Å to find a theoretical transition state that would generate calculated KIEs to best match the experiment determinations (Table 2).

For the GH reaction, a theoretical transition state structure with C−O bond lengths of 2.33 and 2.20 Å to the phosphate leaving group and incoming water nucleophile, respectively, gave the best match between experimental and measured intrinsic KIEs (Figure 5c and Table 2). The [1″-^{14}C] calculated KIE was outside the experimental limits of the intrinsic KIE. However, experimental and calculated [1″-^{14}C] KIEs remains in agreement with a dissociative transition state with oxocarbenium ion character. The C5−O5−C1−C2 glucosyl atoms of the TcdB-GTD GH transition state are in a coplanar arrangement (Figure S7). The best-fit GH transition state from the family of KIEs predict the hexopyranose ring to be in the $^4H_3$ half-chair conformation (Figures S5 and S7).[58] The C4 atom is 0.1 Å above the plane on the β-face while the C3 atom is 0.6 Å below the plane on the α-face. Only the small 2-^{3}H β-secondary KIE is at variance with this transition state, which predicts a $B_{2,5}$ transition state. It is possible that the geometry of the β-secondary C2-^{3}H atom could be influenced by a strong transition state interaction with TcdB-GTD catalytic site amino acids.

Calculation of the TcdB-GTD GT transition state structure fixed the C−O bond between the anomeric carbon and phosphate leaving group at 3.0 Å for the test transition states (*d*1 in Figure 5d). This reflects full loss of the C1-UDP bond to permit initiation of nucleophilic attack from the same face by the Rac1 threonine. The C−O bond distances to the nucleophilic oxygen atom and for proton addition to the leaving group O atom were varied from 1.8−3.0 Å and 2.4−1.0 Å, respectively (*d*2 and *d*3 in Figure 5d). The computed GT transition state that best matched the [1″-^{14}C] and [1″-^{18}O] KIEs had C−O bond lengths of 3.0 Å to the anomeric carbon and an O−H bond length of 2.4 Å for protonation of the phosphate leaving group. Transition state geometry for the TcdB-GTD GT reaction supports an oxocarbenium ion pair at the transition state, causing the glucosyl C5−O5−C1−C2 atoms to be coplanar (Figure S7). The best-fit transition state from the family of KIEs places the hexopyranose ring in an envelope conformation (^{4}E), where the C4 atom is 0.7 Å above the plane on the β-face and the C3 atom is within the plane.[58] Similar to the TcdB-GTD GH transition state, the small

https://doi.org/10.1021/acschembio.2c00408
ACS Chem. Biol. 2022, 17, 2507−2518

experimental α and β secondary KIEs may result from a restricted active site when the UDP leaving group and Rac1 both crowd the same face of the anomeric carbon. These transition state structures were calculated without contributions from the active site amino acid interactions that may influence bond polarization.

Forward motion through the reaction coordinate for the GT reaction is supported by the PIX experiment, revealing an irreversible and/or restricted catalytic environment for the GT reaction, eliminating chemical reversal with torsional β-phosphoryl motion. The theoretical structure most closely related to the KIE constraints (Figure 5d) had imaginary frequencies along the O−H bond corresponding to proton transfer ($d3$) and the C−O bond between the anomeric carbon and the nucleophilic oxygen ($d2$) and is thus not a true transition state structure by the definition of a single imaginary frequency. Accordingly, equilibrium isotope effect (EIE) values were calculated. The intrinsic [1″-^{14}C] KIE matched a calculated EIE of 1.011 between UDP-glucose and the UDP + oxocarbenium ion, where the oxocarbenium ion has a lifetime that is adequate to permit bond vibrational modes to equilibrate. The intrinsic [1″-^{3}H] and [2″-^{3}H] KIEs also matched the calculated EIEs, consistent with a short-lived oxocarbenium ion intermediate. The [1″-^{18}O] calculated EIE was smaller than the experimental KIE, reflecting uncertainty in the degree of protonation for the leaving group oxygen atom.

Electrostatic potential surface (EPS) maps for the optimized TcdB-GTD ground state and GH and GT transition state structures indicate the distribution of partial positive (blue) and partial negative (red) charge (Figure 6). Key features of the TcdB-GTD GH and GT transition states center on the charge distribution around the cationic anomeric carbon of the glucose ring (Figure 6e−i). The positive charge on the anomeric carbon is most pronounced for the TcdB-GTD GT transition state (Figure 6i). Isofagomine, a 2,5 dideoxy-1-imino mimic of glucose, is a nanomolar inhibitor of the TcdA and TcdB toxins and binds only in the presence of UDP[33]. The cationic isofagomine imino group forms a 2.6 Å ion pair with the β-phosphoryl group of UDP to mimic the transition state geometry. An EPS map from the crystal structure of isofagomine-TcdB was also generated (Figure 6j). The positive charge observed at the protonated endocyclic nitrogen atom of isofagomine is isosteric to the positively charged anomeric carbon in the TcdB-GTD GT transition state (Figure 6j).

CONCLUSIONS

Organisms express several hundred glycosyltransferases, a handful of which have been characterized for transition state analysis.[1,2] In contrast, humans express only three UDP-glucose based protein O-glucosyltransferases, and they are also rare in bacterial functions.[59] Mechanistic and KIE analysis of the TcdB-GTD GT transition state expands mechanistic knowledge of the glycosyltransferases to the clinically important bacterial toxins. Knowledge of the transition states for TcdB-GTD glucosyltransferases has also provided the first generation of small molecule inhibitors.

Glucosylation of Rho GTPases by the TcdB toxin from *C. difficile* occurs with overall retention of stereochemistry and KIE measurements support an S_Ni mechanism with a distinct oxocarbenium phosphate ion pair transition state. The glucocation complex has a lifetime long enough to conform to EIE and thus shares characteristics of an intermediate. However, the complex is too transient or too constrained to permit torsional equilibration of the UDP-phosphoryl group. Combined KIE and QM calculations demonstrate that the glycosidic bond to the leaving group is cleaved before the approach of the nucleophilic threonine and that the distances from the anomeric carbon to the leaving group and the nucleophile are large (3.0 Å), indicating the presence of an oxocarbenium ion pair. The TcdB glucosyltransferase is therefore similar to some other retaining glycosyltransferases reported to react by an S_Ni mechanism and ion pair transition states. Enzymes forming glucocation-like transition states are susceptible to inhibition by iminosugar analogues that mimic the cationic nature of the transition state. Thus, isofagomine and noeuromycin mimic the distinct oxocarbenium ion present in the TcdB-GTD GT transition state and are nanomolar inhibitors of the enzyme. The transition state structure of the TcdB glycosyltransferase domain will be useful in designing second-generation transition state analogues toward potential therapeutics for *C. difficile* infections.

ASSOCIATED CONTENT

Supporting Information

The Supporting Information is available free of charge at https://pubs.acs.org/doi/10.1021/acschembio.2c00408.

NMR analysis of stereochemistry of TcdB-GTD glucohydrolase reaction; NMR analysis of TcdB-GTD glucosyltransferase reaction in the presence of 10% methanol; forward commitment (Cf) for TcdB-GTD glucosyltransferase activity; summary of intrinsic KIEs for TcdB-GTD glucosyltransferase reaction and glucohydrolase reaction; conformations for a glucocation; proton inventories for TcdB-GTD glucosyltransferase reaction; calculated TcdB-GTD glucohydrolase and glucosyltransferase transition state structures; and atomic coordinates for QM transition state analysis (PDF)

AUTHOR INFORMATION

Corresponding Author

Vern L. Schramm − *Department of Biochemistry, Albert Einstein College of Medicine, Bronx, New York 10461, United States;* orcid.org/0000-0002-8056-1929; Phone: 718-430-2813; Email: vern.schramm@einsteinmed.edu

Authors

Ashleigh S. Paparella − *Department of Biochemistry, Albert Einstein College of Medicine, Bronx, New York 10461, United States*

Sean M. Cahill − *Department of Biochemistry, Albert Einstein College of Medicine, Bronx, New York 10461, United States*

Briana L. Aboulache − *Department of Biochemistry, Albert Einstein College of Medicine, Bronx, New York 10461, United States;* Present Address: Department of Biochemistry, University of Colorado, Boulder, Colorado, United States (B.L.A.)

Complete contact information is available at: https://pubs.acs.org/10.1021/acschembio.2c00408

Author Contributions

A.S.P. performed synthesis of UDP-glucose substrates, preparation of all NMR samples, KIE analysis of TcdB-GTD

https://doi.org/10.1021/acschembio.2c00408
ACS Chem. Biol. 2022, 17, 2507−2518

catalyzed reaction, and QM calculations on TCdB-GTD catalyzed reactions. S.M.C. acquired and helped to analyze all NMR data. B.L.A. performed kinetic analysis of TcdB-GTD glucosyltransferase reaction and performed Lineweaver−Burk analysis. V.L.S. designed and supervised the project. All authors contributed to writing the manuscript. All authors have given approval to the final version of the manuscript.

Funding

This work was supported by NIH research grants GM041916 and AI150971. The Bruker 600 MHz NMR instrument in the structural NMR resource at the Albert Einstein College of Medicine was purchased using funds from NIH award 1S10OD016305 and is supported by a Cancer Center Support Grant (P30CA013330).

Notes

The authors declare no competing financial interest.

■ ACKNOWLEDGMENTS

The authors thank P. Tyler for providing α-glucosylated threonine for NMR measurements and M. Brown and G. Bedard for helpful discussions with the QM calculations.

■ ABBREVIATIONS

GT glucosyltransferase
GH glucohydrolase
KIE kinetic isotope effect
QM quantum mechanics
EIE equilibrium isotope effect.

■ REFERENCES

(1) Lairson, L. L.; Henrissat, B.; Davies, G. J.; Withers, S. G. Glycosyltransferases: Structures, functions, and mechanisms. *Annu. Rev. Biochem.* **2008**, *77*, 521−555.
(2) Breton, C.; Fournel-Gigleux, S.; Palcic, M. M. Recent structures, evolution and mechanisms of glycosyltransferases. *Curr. Opin. Struct. Biol.* **2012**, *22*, 540−549.
(3) Kim, S. C.; Singh, A. N.; Raushel, F. M. Analysis of the galactosyltransferase reaction by positional isotope exchange and secondary deuterium isotope effects. *Arch. Biochem. Biophys.* **1988**, *267*, 54−59.
(4) Bruner, M.; Horenstein, B. A. Isotope trapping and kinetic isotope effect studies of rat liver alpha-(2−>6)-sialyltransferase. *Biochemistry* **1998**, *37*, 289−297.
(5) Ardevol, A.; Iglesias-Fernandez, J.; Rojas-Cervellera, V.; Rovira, C. The reaction mechanism of retaining glycosyltransferases. *Biochem. Soc. Trans.* **2016**, *44*, 51−60.
(6) Gibson, R. P.; Lloyd, R. M.; Charnock, S. J.; Davies, G. J. Characterization of *Escherichia coli* OtsA, a trehalose-6-phosphate synthase from glycosyltransferase family 20. *Acta Crystallogr. D Biol. Crystallogr.* **2002**, *58*, 349−351.
(7) Persson, K.; Ly, H. D.; Dieckelmann, M.; Wakarchuk, W. W.; Withers, S. G.; Strynadka, N. C. Crystal structure of the retaining galactosyltransferase LgtC from *Neisseria meningitidis* in complex with donor and acceptor sugar analogs. *Nat. Struct. Biol.* **2001**, *8*, 166−175.
(8) Jamaluddin, H.; Tumbale, P.; Withers, S. G.; Acharya, K. R.; Brew, K. Conformational changes induced by binding UDP-2F-galactose to alpha-1,3 galactosyltransferase- implications for catalysis. *J. Mol. Biol.* **2007**, *369*, 1270−1281.
(9) Vetting, M. W.; Frantom, P. A.; Blanchard, J. S. Structural and enzymatic analysis of MshA from *Corynebacterium glutamicum*: substrate-assisted catalysis. *J. Biol. Chem.* **2008**, *283*, 15834−15844.
(10) Reinert, D. J.; Jank, T.; Aktories, K.; Schulz, G. E. Structural basis for the function of *Clostridium difficile* toxin B. *J. Mol. Biol.* **2005**, *351*, 973−981.
(11) Albesa-Jove, D.; Mendoza, F.; Rodrigo-Unzueta, A.; Gomollon-Bel, F.; Cifuente, J. O.; Urresti, S.; Comino, N.; Gomez, H.; Romero-Garcia, J.; Lluch, J. M.; Sancho-Vaello, E.; Biarnes, X.; Planas, A.; Merino, P.; Masgrau, L.; Guerin, M. E. A native ternary complex trapped in a crystal reveals the catalytic mechanism of a retaining glycosyltransferase. *Angew. Chem., Int. Ed.* **2015**, *54*, 9898−9902.
(12) Sinnott, M. L. Catalytic mechanism of enzymic glycosyl transfer. *Chem. Rev.* **1990**, *90*, 1171−1202.
(13) Sinnott, M. L.; Jencks, W. P. Solvolysis of D-glucopyranosyl derivatives in mixtures of ethanol and 2,2,2-trifluoroethanol. *J. Am. Chem. Soc.* **1980**, *102*, 2026−2032.
(14) Klein, H. W.; Im, M. J.; Palm, D. Mechanism of the phosphorylase reaction. *Eur. J. Biochem.* **1986**, *157*, 107−114.
(15) Chan, J.; Tang, A.; Bennet, A. J. A stepwise solvent-promoted SNi reaction of α-d-glucopyranosyl fluoride: mechanistic implications for retaining glycosyltransferases. *J. Am. Chem. Soc.* **2012**, *134*, 1212−1220.
(16) Lee, S. S.; Hong, S. Y.; Errey, J. C.; Izumi, A.; Davies, G. J.; Davis, B. G. Mechanistic evidence for a front-side, SNi-type reaction in a retaining glycosyltransferase. *Nat. Chem. Biol.* **2011**, *7*, 631−638.
(17) Ardevol, A.; Rovira, C. The molecular mechanism of enzymatic glycosyl transfer with retention of configuration: evidence for a short-lived oxocarbenium-like species. *Angew. Chem., Int. Ed.* **2011**, *50*, 10897−10901.
(18) Bobovska, A.; Tvaroska, I.; Kona, J. A theoretical study on the catalytic mechanism of the retaining alpha-1,2-mannosyltransferase Kre2p/Mnt1p: the impact of different metal ions on catalysis. *Org. Biomol. Chem.* **2014**, *12*, 4201−4210.
(19) Gomez, H.; Rojas, R.; Patel, D.; Tabak, L. A.; Lluch, J. M.; Masgrau, L. A computational and experimental study of O-glycosylation. Catalysis by human UDP-GalNAc polypeptide:GalNAc transferase-T2. *Org. Biomol. Chem.* **2014**, *12*, 2645−2655.
(20) Ferreira, P.; Fernandes, P. A.; Ramos, M. J. The catalytic mechanism of the retaining glycosyltransferase mannosylglycerate synthase. *Chemistry* **2021**, *27*, 13998−14006.
(21) Gomez, H.; Polyak, I.; Thiel, W.; Lluch, J. M.; Masgrau, L. Retaining glycosyltransferase mechanism studied by QM/MM methods: lipopolysaccharyl-alpha-1,4-galactosyltransferase C transfers alpha-galactose via an oxocarbenium ion-like transition state. *J. Am. Chem. Soc.* **2012**, *134*, 4743−4752.
(22) Voth, D. E.; Ballard, J. D. *Clostridium difficile* toxins: mechanism of action and role in disease. *Clin. Microbiol. Rev.* **2005**, *18*, 247−263.
(23) Aktories, K. Bacterial protein toxins that modify host regulatory GTPases. *Nat. Rev. Microbiol.* **2011**, *9*, 487−498.
(24) Aktories, K.; Schwan, C.; Jank, T. *Clostridium difficile* Toxin Biology. *Ann. Rev. Microbiol.* **2017**, *71*, 281−307.
(25) Markham, A. Bezlotoxumab: First global approval. *Drugs* **2016**, *76*, 1793−1798.
(26) Bender, K.; Garland, M.; Ferreyra, J. A.; Hryckowian, A. J.; Child, M. A.; Puri, A. W.; Solow-Cordero, D. E.; Higginbottom, S. K.; Segal, E.; Banaei, N.; Shen, A.; Sonnenburg, J. L.; Bogyo, M. A small-molecule antivirulence agent for treating *Clostridium difficile* infection. *Sci. Transl. Med.* **2015**, *7*, 306ra148.
(27) Letourneau, J. J.; Stroke, I. L.; Hilbert, D. W.; Cole, A. G.; Sturzenbecker, L. J.; Marinelli, B. A.; Quintero, J. G.; Sabalski, J.; Li, Y.; Ma, L.; Pechik, I.; Stein, P. D.; Webb, M. L. Synthesis and SAR studies of novel benzodiazepinedione-based inhibitors of *Clostridium difficile* (*C. difficile*) toxin B (TcdB). *Bioorg. Med. Chem. Lett.* **2018**, *28*, 3601−3605.
(28) Tam, J.; Hamza, T.; Ma, B.; Chen, K.; Beilhartz, G. L.; Ravel, J.; Feng, H.; Melnyk, R. A. Host-targeted niclosamide inhibits *C. difficile* virulence and prevents disease in mice without disrupting the gut microbiota. *Nat. Commun.* **2018**, *9*, 5233.
(29) Drula, E.; Garron, M. L.; Dogan, S.; Lombard, V.; Henrissat, B.; Terrapon, N. The carbohydrate active enzyme database: functions and literature. *Nucleic Acids Res.* **2022**, *50*, D571−D577.

https://doi.org/10.1021/acschembio.2c00408
ACS Chem. Biol. 2022, 17, 2507−2518

(30) Genth, H.; Schelle, I.; Just, I. Metal Ion Activation of Clostridium sordellii Lethal Toxin and Clostridium difficile Toxin B. *Toxins (Basel)* **2016**, *8*, 109.
(31) Jank, T.; Giesemann, T.; Aktories, K. *Clostridium difficile* glucosyltransferase toxin B-essential amino acids for substrate binding. *J. Biol. Chem.* **2007**, *282*, 35222−35231.
(32) Ciesla, W. P., Jr.; Bobak, D. A. *Clostridium difficile* toxins A and B are cation-dependent UDP-glucose hydrolases with differing catalytic activities. *J. Biol. Chem.* **1998**, *273*, 16021−16026.
(33) Paparella, A. S.; Aboulache, B. L.; Harijan, R. K.; Potts, K. S.; Tyler, P. C.; Schramm, V. L. Inhibition of *Clostridium difficile* TcdA and TcdB toxins with transition state analogues. *Nat. Commun.* **2021**, *12*, 6285.
(34) Tam, J.; Beilhartz, G. L.; Auger, A.; Gupta, P.; Therien, A. G.; Melnyk, R. A. Small molecule inhibitors of *Clostridium difficile* toxin B-induced cellular damage. *Chem. Biol.* **2015**, *22*, 175−185.
(35) Risley, J. M.; Van Etten, R. L. Kinetics of oxygen exchange at the anomeric carbon atom of D-glucose and D-erythrose using the oxygen-18 isotope effect in carbon-13 nuclear magnetic resonance spectroscopy. *Biochemistry* **1982**, *21*, 6360−6365.
(36) Bensadoun, A.; Weinstein, D. Assay of proteins in the presence of interfering materials. *Anal. Biochem.* **1976**, *70*, 241−250.
(37) Rose, I. A. The isotope trapping method: desorption rates of productive E.S complexes. *Methods Enzymol.* **1980**, *64*, 47−59.
(38) Frisch, M. J.; Trucks, G. W.; Schlegel, H. B.; Scuseria, G. E.; Robb, M. A.; Cheeseman, J. R.; Scalmani, G.; Barone, V.; Petersson, G. A.; Nakatsuji, H.; Caricato, M.; Li, X.; Hratchian, H.P.; Izmaylov, A.F.; Bloino, J.; Zheng, G.; Sonnenberg, J.L.; Hada, M.; Ehara, M.; Toyota, K.; Fukuda, R.; Hasegawa, J.; Ishida, M.; Nakajima, T.; Honda, Y.; Kitao, O.; Nakai, H.; Vreven, T.; Montgomery, J.A., Jr.; Peralta, J.E.; Ogliaro, F.; Bearpark, M.; Heyd, J.J.; Brothers, E.; Kudin, K.N.; Staroverov, V.N.; Kobayashi, R.; Normand, J.; Raghavachari, K.; Rendell, A.; Burant, J.C.; Iyengar, S.S.; Tomasi, J.; Cossi, M.; Rega, N.; Millam, N.J.; Klene, M.; Knox, J.E.; Cross, J.B.; Bakken, V.; Adamo, C.; Jaramillo, J.; Gomperts, R.; Stratmann, R.E.; Yazyev, O.; Austin, A. J.; Cammi, R.; Pomelli, C.; Ochterski, J. W.; Martin, R.L.; Morokuma, K.; Zakrzewski, V.G.; Voth, G.A.; Salvador, P.; Dannenberg, J.J.; Dapprich, S.; Daniels, A.D.; Farkas, Ö.; Foresman, J.B.; Ortiz, J.V.; Cioslowski, J.; Fox, D.J. *Gaussian 09 Rev. C.01*; Wallingford, CT, 2009.
(39) Anisimov, V.; Paneth, P. ISOEFF98. A program for studies of isotope effects using Hessian modifications. *J. Math. Chem.* **1999**, *26*, 75−86.
(40) Dona, A. C.; Pages, G.; Kuchel, P. W. Kinetics of starch hydrolysis and glucose mutarotation studied by NMR chemical exchange saturation transfer (CEST). *Carbohydr. Polym.* **2011**, *86*, 1525−1532.
(41) Flood, A. E.; Srisa-nga, S. Mutarotation rates and equilibrium of simple carbohydrates. *Asian Pacific. Confed. Chem. Eng. Congr. Progr. Abstr.* **2004**, *113*, 1−10.
(42) Schache, D.; Bardin, S.; Ciobanu, L.; Faber, C.; Hoerr, V. Ultrafast CEST line scanning as a method to quantify mutarotation kinetics. *J. Magn. Reson.* **2022**, *342*, No. 107270.
(43) Lewis, B. E.; Choytun, N.; Schramm, V. L.; Bennet, A. J. Transition states for glucopyranose interconversion. *J. Am. Chem. Soc.* **2006**, *128*, 5049−5058.
(44) Geyer, M.; Wilde, C.; Selzer, J.; Aktories, K.; Kalbitzer, H. R. Glucosylation of Ras by *Clostridium sordellii* lethal toxin: Consequences for effector loop conformations observed by NMR spectroscopy. *Biochemistry* **2003**, *42*, 11951−11959.
(45) Vetter, I. R.; Hofmann, F.; Wohlgemuth, S.; Herrmann, C.; Just, I. Structural consequences of mono-glucosylation of Ha-Ras by *Clostridium sordellii* lethal toxin. *J. Mol. Biol.* **2000**, *301*, 1091−1095.
(46) Copeland, R. A., *Enzymes: A practical Introduction to Structure, Mechanism, and Data Analysis*; Wiley-WCH: 2000.
(47) D'Urzo, N.; Malito, E.; Biancucci, M.; Bottomley, M. J.; Maione, D.; Scarselli, M.; Martinelli, M. The structure of *Clostridium difficile* toxin A glucosyltransferase domain bound to Mn^{2+} and UDP provides insights into glucosyltransferase activity and product release. *FEBS J.* **2012**, *279*, 3085−3097.
(48) Liu, Z.; Zhang, S.; Chen, P.; Tian, S.; Zeng, J.; Perry, K.; Dong, M.; Jin, R. Structural basis for selective modification of Rho and Ras GTPases by *Clostridioides difficile* toxin B. *Sci. Adv.* **2021**, *7*, No. eabi4582.
(49) Kim, S. C.; Singh, A. N.; Raushel, F. M. The mechanism of glycogen synthetase as determined by deuterium isotope effects and positional isotope exchange experiments. *J. Biol. Chem.* **1988**, *263*, 10151−10154.
(50) Singh, A. N.; Hester, L. S.; Raushel, F. M. Examination of the mechanism of sucrose synthetase by positional isotope exchange. *J. Biol. Chem.* **1987**, *262*, 2554−2557.
(51) Northrop, D. B. On the meaning of K_m and V/K in enzyme kinetics. *J. Chem. Educ.* **1998**, *75*, 1153−1157.
(52) Schramm, V. L. Enzymatic transition-state analysis and transition-state analogs. *Methods Enzymol.* **1999**, *308*, 301−355.
(53) Berti, P. J.; McCann, J. A. B. Toward a detailed understanding of base excision repair enzymes: transition state and mechanistic analyses of N-glycoside hydrolysis and N-glycoside transfer. *Chem. Rev.* **2006**, *106*, 506−555.
(54) Rosenberg, S.; Kirsch, J. F. Oxygen-18 leaving group kinetic isotope effects on the hydrolysis of nitrophenyl glycosides. 2. Lysozyme and beta-glucosidase: acid and alkaline hydrolysis. *Biochemistry* **1981**, *20*, 3196−3204.
(55) Schramm, V. L. Enzymatic transition states and transition state analog design. *Annu. Rev. Biochem.* **1998**, *67*, 693−720.
(56) Sunko, D. E.; Hirsl-Starcevic, S.; Pollack, S. K.; Hehre, W. J. Hyperconjugation and homohyperconjugation in the 1-adamantyl cation. Qualitative models for. gamma.-deuterium isotope effects. *J. Am. Chem. Soc.* **1979**, *101*, 6163−6170.
(57) Berti, P. J.; Tanaka, K. S. E. Transition state analysis using multiple kinetic isotope effects: mechanisms of enzymatic and non-enzymatic glycoside hydrolysis and transfer. *Adv. Phys. Org. Chem.* **2002**, *37*, 239−314.
(58) Davies, G. J.; Planas, A.; Rovira, C. Conformational analyses of the reaction coordinate of glycosidases. *Acc. Chem. Res.* **2012**, *45*, 308−316.
(59) Mehboob, M. Z.; Lang, M. Structure, function, and pathology of protein O-glucosyltransferases. *Cell Death Dis.* **2021**, *12*, 1−13.

https://doi.org/10.1021/acschembio.2c00408
ACS Chem. Biol. 2022, 17, 2507−2518